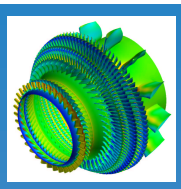

NONLINEAR FREQUENCY DOMAIN METHOD

Matthew McMullen, Arathi Gopinath, Antony Jameson and Juan Alonso
Stanford University

Motivation

- TFLO has access to a variety of ASCI computational facilities. Different processor/machine combinations affect the overall execution time, but estimates for job length are now provided in months/years.

Component	Blade Rows	Grid Points (million)	% Wheel	Total CPU Hours (million)	Execution Time
Turbine	9	94	16	3.0	510 days[1]
Compressor	23	N/A	16	7.7	1300 days[1]

[1] Estimates based on 500-1000 processors at 8 hours per day.

- TFLO is currently based on a fully implicit dual time stepping algorithm utilizing a nested system of loops. The outer iteration advances the solution forward in physical time, while the inner iterations minimize the residual at each time step.
- The figure to the right plots the inlet mass fluctuation as a function of time step for the Aachen test case. A time accurate solver is at a disadvantage, because the time scale of the periodic solution is much smaller than the time scale of the decay of the initial transients.

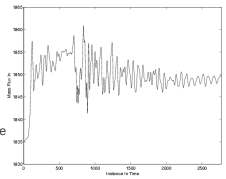

Non-Linear Equations Recast in the Frequency Domain

- The Navier-Stokes equations can be expressed in simplified form.

$$\frac{\partial w}{\partial t} + \frac{\partial}{\partial x} f(w) + \frac{\partial}{\partial y} g(w) = 0$$

- Using finite volume techniques the above equation can be rewritten as the sum of volumetric and surface integrals. Approximating the volumetric integral as the product of the cell volume and the time derivative, the above equation can be written in a simplified form.

$$V \frac{\partial W}{\partial t} + R(W) = 0$$

- Assuming that the solution and residual are periodic over the same time period, the above equation can be recast into the frequency domain. Adding in a pseudo time derivative term allows us to march this transformed system forward to a periodic steady state.

$$V \frac{d\hat{W}_k}{d\tau} + ikV\hat{W}_k + \hat{R}_k = 0$$

- The non-linear residual term is calculated in physical space and time. The term is transformed to the frequency domain using a Fast Fourier Transform. A typical solution iteration implements the following data flow diagram.

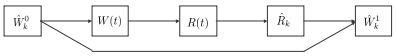

Gradient Based Variable Time Period

- The representation of the solution or residual in the form of a Fourier series makes an assumption of the time period of the fundamental harmonic. A class of problems exist where the time period of the discrete equations is unknown. To determine its value we pose an optimization problem where the time period is adjusted to minimize the magnitude of the unsteady residual.
- The unsteady residual is written as a function of the time period.

$$\hat{I}_n = -V \frac{d\hat{W}_n}{d\tau} = \frac{i2\pi nV}{T} \hat{W}_n + \hat{R}_n$$

- A gradient of the magnitude of the unsteady residual with respect to the time period can be determined.

$$\frac{1}{2} \frac{\partial \left| \hat{I}_n \right|^2}{\partial T} = \hat{I}_{nr} \frac{\partial \hat{I}_{nr}}{\partial T} + \hat{I}_{ni} \frac{\partial \hat{I}_{ni}}{\partial T}$$

$$\frac{\partial \hat{I}_{nr}}{\partial T} = \frac{2\pi nV \hat{W}_{ni}}{T^2} \qquad \frac{\partial \hat{I}_{ni}}{\partial T} = -\frac{2\pi nV \hat{W}_{nr}}{T^2}$$

- The gradient adjusts the time period at the end of each multigrid cycle.

$$T^{n+1} = T^n - \Delta T \frac{\partial \left| \hat{I}_n \right|^2}{\partial T}$$

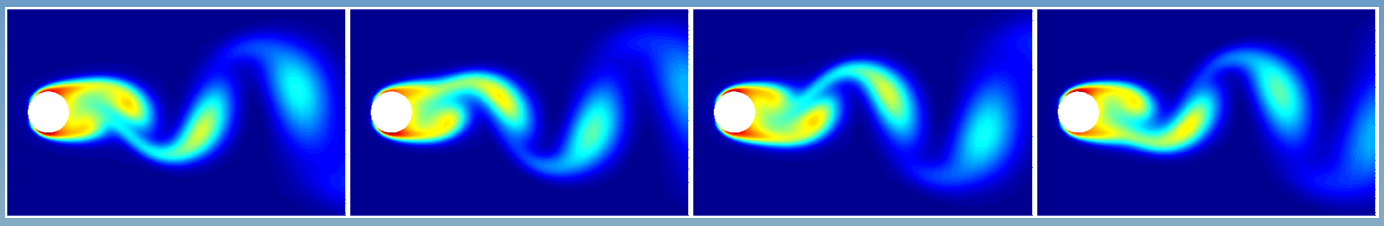

Cylinder Strouhal Results

- An unsteady wake of shedding vortices naturally appears behind a cylinder between a Reynolds number of 49 and 194. Numerical simulations of this flow were performed using 4 different meshes (129x65, 193x81, 257x129 and 385x161) and 4 different temporal resolutions.
- Using the GBVTP method, the shedding frequency can be predicted. The right hand figure shows the numerical prediction of the Strouhal number as a function of Reynolds number and compares these results to experiments and other calculations.

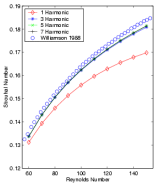

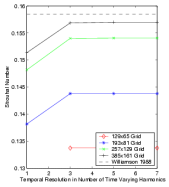

- The left hand figure shows the variation in the Strouhal number over different temporal resolutions. The results converge to an invariant answer between one and three modes.

Cylinder Base Suction Coefficient Results

- The mean base suction coefficient is a common figure of merit used by experimentalists and numericists studying this problem. From a numerical viewpoint, this coefficient is sensitive to artificial dissipation injected into the spatial and temporal discretizations.
- The figure to the right shows the numerical predictions for this coefficient as a function of Reynolds number. Results are plotted for a variety of spatial resolutions and compared to experimental and other numerical results.

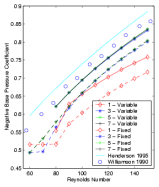

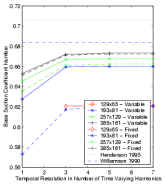

- The figure to the left shows the suction coefficient results for two different sets of calculations: fixed time period and GBVTP. It is inferred that the variable time period method has a positive impact on the suction coefficient.

Convergence

- The convergence rate of the NLFD code is comparable with the state of the art in steady solvers.
- The figure to the right plots the magnitude of the residual versus the multigrid cycle used in the solution process. All of the harmonics within the residual decay consistently with a similar FLO103 calculation.

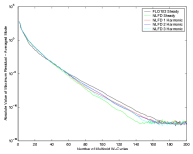

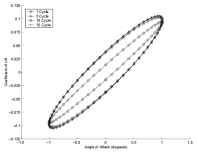

- The figure to the left shows that 10-15 multigrid cycles are required to converge coefficient of lift predictions from an unsteady Euler calculation to plotting accuracy. Turbulent Navier-Stokes results at equivalent farfield conditions converge to similar accuracy between 50 and 60 cycles.

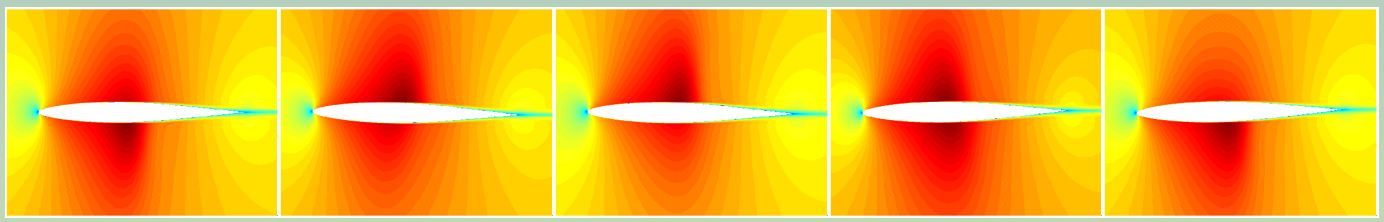

Pitching Airfoil - Inviscid

- An Euler calculation was performed simulating the Landon 0012 unsteady experiment published in AGARD-702. The airfoil rotated ±2.41 degrees about a mean angle of attack of 2.89 degrees. A farfield Mach number of 0.6 created transonic effects throughout the rotation of the foil.
- The figure to the right compares coefficient of lift results provided by experiment and Euler simulations using time accurate and NLFD codes. The numerical simulations agree closely using just one temporal mode.

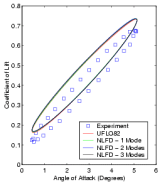

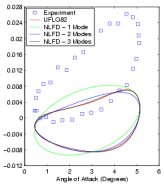

- The figure to the left compares coefficient of moment results provided by experiment and Euler simulations using time accurate and NLFD codes. The numerical results agree closely with each other but significantly diverge from experimental results.

Pitching Airfoil - Viscous

- A viscous calculation of the Landon 0012 unsteady experiment was performed on a 513x97 mesh. The Baldwin-Lomax turbulence model was implemented using a snapshot approach, essentially ignoring the unsteady effects on the turbulence field.
- Comparison of the coefficient of lift versus angle of attack using both numerical simulations and experiment is provided in the figure to the right. The viscous terms effectively reduce the mean lift curve slope providing excellent agreement between results.

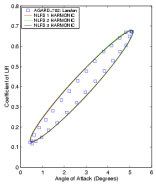

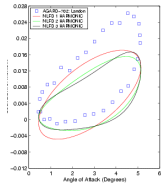

- Comparison of the coefficient of moment versus angle of attack using both numerical simulations and experiment is provided in the figure to the left. A significant difference exists between results regardless of temporal resolution.

Conclusions and Future Work

- The numerical results confirm the accuracy and computational efficiency of the Nonlinear Frequency Domain (NLFD) method.
- Cylinder Results:
  - NLFD predictions of the mean base suction coefficient agreed closely with experimental data using just three temporal modes.
  - The time period of the fundamental harmonic can be accurately predicted using the Gradient Based Variable Time Period method.
- Pitching Airfoil Results:
  - RANS simulations using the NLFD code provided coefficient of lift results that agreed closely with experimental data using only one temporal mode.
  - Regardless of the governing equations, NLFD predictions of the coefficient of moment had poor agreement with experimental results.
- Work has been started to apply the NLFD method in the turbomachinery environment. Due to the geometric complexity, the number of temporal modes and hence the computational cost may increase. If this number grows above a certain threshold, then time accurate solvers may regain an advantage in terms of computational cost.